magnetism

MDPI

Article

Application of Magnetic Separation in Catalyst Reuse Applied in Paracetamol Degradation

Jessica R. P. Oliveira [1], Eduardo Abreu [2], Maria E. K. Fuziki [2], Elaine T. de Paula [3], Michel Z. Fidelis [2], Rodrigo Brackmann [4], Angelo M. Tusset [1], Odivaldo C. Alves [5] and Giane G. Lenzi [1,3,*]

1 Department of Production Engineering, Federal University of Technology-Paraná, Paraná-Rua Doutor Washington Subtil Chueire, 330, Ponta Grossa 84017-220, Brazil; jessica_do_rocio@hotmail.com (J.R.P.O.); tusset@utfpr.edu.br (A.M.T.)
2 Department of Chemical Engineering, State University of Maringá, Colombo Ave. 5790, Maringá 87020-900, Brazil; eduardo_abreu@live.com (E.A.); mariafuziki@alunos.utfpr.edu.br (M.E.K.F.); michelmzzf@gmail.com (M.Z.F.)
3 Department of Chemical Engineering, Federal University of Technology-Paraná, Paraná-Doutor Washington Subtil Chueire St., 330, Ponta Grossa 84017-220, Brazil; elainetrojanpaula@alunos.utfpr.edu.br
4 Department of Chemical, Federal University of Technology-Paraná, Via do Conhecimento, s/n—km 01, Pato Branco 85503-390, Brazil; rodrigobrackmann@utfpr.edu.br
5 Department of Chemistry, Institute of Chemistry, Federal Fluminense University, R. Outeiro de S. J. Batista s/n, Niterói 24020-150, Brazil; odivaldocambraia@id.uff.br
* Correspondence: gianeg@utfpr.edu.br

Abstract: This work presents an investigation of the degradation of paracetamol via heterogeneous photocatalysis, aiming to magnetically immobilize the catalyst in a continuous process. Catalyst immobilization was conducted on aggregated flower-like structures. The $CoFe_2O_4$@Nb_5O_2 catalyst was characterized using a Vibrating Sample Magnetometer (VSM). The effects of the magnetic immobilization of the catalyst, flow, residence time, adsorption, and photolysis were evaluated. Additionally, catalyst reuse cycles were analyzed. The results indicated that a longer residence time favors the degradation of paracetamol due to the increase in the contact time of the effluent catalyst. At a flow rate of 20 mL·min^{-1}, a degradation of 27% was obtained. Photolysis and adsorption tests indicated that residence time was not an important factor for paracetamol degradation. For the photolysis test, in the first cycle, the values obtained were in the range of 6.0–8.5%. The adsorption results indicated ~10% removal.

Keywords: emerging pollutants; photocatalysis; continuous process

Citation: Oliveira, J.R.P.; Abreu, E.; Fuziki, M.E.K.; Paula, E.T.d.; Fidelis, M.Z.; Brackmann, R.; Tusset, A.M.; Alves, O.C.; Lenzi, G.G. Application of Magnetic Separation in Catalyst Reuse Applied in Paracetamol Degradation. *Magnetism* **2024**, *4*, 240–251. https://doi.org/10.3390/magnetism4030016

Academic Editors: Gerardo F. Goya, Andrea Atrei and Łukasz Hawełek

Received: 31 January 2024
Revised: 7 July 2024
Accepted: 1 August 2024
Published: 12 August 2024

1. Introduction

In recent years, due to the emergence of new analysis technologies, the low efficiency of effluent treatment systems, and the increasing use of chemical compounds, new substances are being identified. Among these, the so-called emerging contaminants (ECs) stand out, which are found in products for domestic and industrial use. Pharmaceuticals, in particular, are released in large quantities into the environment, posing a great risk to aquatic biota and exposed living beings.

Some methods have been used to treat water containing ECs, such as adsorption [1], activated sludge treatment, membrane bioreactors [2], reverse osmosis [1], and advanced oxidative processes (AOPs) [3]. AOPs are characterized by being able to transform organic contaminants into carbon dioxide, water, and inorganic anions through degradation reactions that involve transient oxidizing species. They are clean and non-selective processes and can be used to degrade organic compounds in both the aqueous and gaseous phases.

The process of catalysis is the main principle of the principles of green chemistry (PGC) [4]. Catalysts are crucial in modern chemical processes, enabling efficient and selective reactions while reducing energy consumption and waste generation [5]. But it is

better that the catalyst chosen can be environmentally friendly and ideally can be recovered after the reaction, and not be one more form of waste after the synthesis [6]. Among the numerous applications of catalysts, the degradation of pharmaceutical compounds is frequently studied [7–11].

Heterogeneous photocatalysis, in particular, is a technology that has been explored to remove emerging polluting compounds [12]. This technology can promote the complete degradation of organic pollutants to CO_2, H_2O, and ions. The process involves the activation of a semiconductor material such as TiO_2, ZnO, ZrO_2, SnO_2, CeO_2, CdS, and ZnS via sunlight or artificial light. Niobium pentoxide (Nb_2O_5) has been used as an alternative to these catalysts in photocatalytic processes, as it has characteristics very similar to those of TiO_2 and greater accessibility.

However, the stage of separating the photocatalyst in suspension at the end of the process is one of the major obstacles to the application of photocatalysis on a large scale, given the costs and difficulties involved [5]. In this sense, the immobilization of photocatalysts has proven to be an interesting alternative that facilitates the separation step and the carrying out of the photocatalytic process in continuous flow [13].

The other important aspect in the field of catalysts is their recovery and reuse, which minimizes costs and reduces the environmental footprint of chemical processes [9,14–16]. Traditional catalyst recovery methods often involve complex procedures, leading to inefficiencies and wasted resources, such as water and energy. This highlights the need for innovative approaches to catalyst recovery, such as magnetic separation, which has been studied so much in the last few years [9,14–16].

Magnetic separation has emerged as a promising technique for recovering catalysts due to its simplicity, efficiency, and environmental friendliness. By taking advantage of the magnetic properties of certain materials, this method allows for the selective separation of catalysts from reaction mixtures, facilitating their reuse with minimal loss or contamination [9,14–16].

In this study, through addressing key issues related to catalyst recovery and reuse, we aim to contribute to the advancement of environmentally friendly solutions for drug contamination in wastewater treatment. In this context, the contribution of the present study was to use a $CoFe_2O_4$@Nb_5O_2 magnetic catalyst, characterize its properties, and apply it to the degradation of paracetamol in a continuous process. The process used to degrade the pollutant was photocatalysis. The parameters analyzed were pH, flow rate (residence time), and use cycles (reuse). In addition, experiments were carried out to verify the adsorption and photolysis influence.

2. Materials and Methods

2.1. Chemicals

Acetonitrile (CH_3CN), supplied by Merck S/A, Parque Rincão-SP, Brazil; anhydrous sodium sulfate (Na_2SO_4), supplied by Neon, Suzano-SP, Brazil; cobalt nitrate ($Co(NO_3)_2{\cdot}6H_2O$), supplied by Synth, Diadema-SP, Brazil; hydrochloric acid (HCl, 37%), supplied by VWR chemicals, São Paulo-SP, Brazil; iron nitrate ($Fe(NO_3)_3{\cdot}9H_2O$), supplied by Synth, Diadema-SP, Brazil; niobium pentoxide (Nb_2O_5), supplied by CBMM—Companhia Brasileira de Metalurgia e Mineração, Araxá-MG, Brazil; sodium hydroxide (NaOH), supplied by Dinâmica Química Contemporânea Ltd.a., Indaiatuba-SP, Brazil; sulfuric acid (H_2SO_4), supplied by Dinâmica Química Contemporânea Ltd.a., Indaiatuba-SP, Brazil.

2.2. Catalysts

According to Oliveira et al. (2023) [17], the first step to obtaining the catalyst is obtaining the citrus fruit extract and storing it in a freezer until use. In the second step, the cobalt ferrite functionalized in niobium pentoxide ($CoFe_2O_4$@Nb_2O_5) is synthesized. The salts Fe^{3+} (11.4 mmol) and Co^{2+} (5.7 mmol) were weighed in an Erlenmeyer flask. After 25 mL of extract (obtained in the first step) was added, the resultant solution immediately showed a black color. The contents of the Erlenmeyer flask were stirred at 200 $\pm$ 2 rpm and

298 ± 2 K for 15 min. Sequentially, 1.33 g of niobium pentoxide was weighed and added to the Erlenmeyer. The mixture was stirred for more than 15 min under the same conditions. In sequence, the mixture was transferred to a porcelain crucible. After, the mixture was dried for 4.5 h at 373 ± 10 K until forming a gel. Finally, the porcelain crucible with the gel was calcined until it reached 873 K. After calcination, the resulting material in the porcelain crucible is cobalt ferrite functionalized in niobium (CFNb) [17].

2.3. Characterization Techniques

In a previous work, the CFNb nanoparticles were characterized via different techniques, such as Photoacoustic Spectroscopy, Point of Zero Charge (pHpzc), Scanning Electron Microscopy (SEM), Energy Dispersive Spectroscopy (EDS), X-ray Diffraction (XRD), and Analysis and Transmission Electron Microscopy (TEM) [17]. In our study, one more characterization was performed; the Vibrating Sample Magnetometer (VSM) analysis.

Catalyst samples were diluted in 80% silica (quartz powder) because the color was too dark for analysis without dilution. Photoacoustic spectroscopy was performed under conditions of 200–700 nm, 800 W, and 23 Hz. pH_{PZC} tests were performed according to the methodologies of the authors Ibrahim et al. (2020) and Oliveira et al. (2021) [18,19].

The SEM images were obtained using the scanning electron microscope model VEGA 3 LMU brand TESCAN, completed with a W 20 kV filament, a 3.0 nm resolution, retractable SE and BSE detectors, a low-vacuum mode (500 Pa) chamber with an internal diameter of 230 mm and a door opening of 148 mm, a 5-axis compucentric stage; the microscope was fully motorized, with X: 80 mm, Y: 60 mm, and Z: 47 mm movements, a CCD camera for viewing the sample chamber and "chamberview" software, VegaTC operating software, a data processing system, and a track ball. The microscope also had an EDS Detector, model AZTec Energy X-Act, resolution 130 eV, Oxford.

The X-ray diffractograms of the samples were obtained using a Rigaku diffractometer model Miniflex 600 with copper radiation (CuKα λ = 1.54 Å) in the Bragg angle range of $3° \leq 2\theta \leq 90°$, with a step of 0.05°, and time fixed count of 2 s per step in a semi-continuous mode. The signals emitted are given as an intensity graph, whose unit is expressed in counts per second (cps) as a function of the scanning angle (2θ, or Bragg angle). The transmission electron microscopy (TEM) images were obtained to verify their morphology with the help of a microscope (JOEL JEM-1250) of 120 kV.

Finally, one more characterization was performed; the magnetization measurements as a function of the field were carried out at 300 K in the range of −20,000 G to 20,000 G using the VSM (Vibrating Sample Magnetometer) mode of the PPMS (Physical Property Measurements System) equipment model Versalab from Quantum Design.

2.4. Photocatalysis

The first step to carry out photocatalysis in continuous flow was choosing the glass tubular reactor and establishing the distance between the magnets; Figure 1a. Next, a system was assembled supporting the reactor on the bar containing the magnets; Figure 1b. Subsequently, the mercury lamp was placed on the system, and it was isolated with a reflective material (aluminum) to avoid dissipation and thus make better use of the luminosity for photocatalysis; Figure 1c. With the system's base assembled, 2.5 g of magnetic catalyst was placed inside the reactor and distributed over the magnets in a flower format (Figure 2) due to magnetic attraction; Figure 1d. Finally, the reactor was connected to a peristaltic pump to regulate the inlet flow of the solution containing paracetamol (20 $mg{\cdot}L^{-1}$); Figure 1e. The flow rates studied were 2.84, 5.77, and 8.63 mL min-120, and the residence times were approximately 13, 27, and 54 min, respectively. The effects of the photolysis and adsorption process were also evaluated.

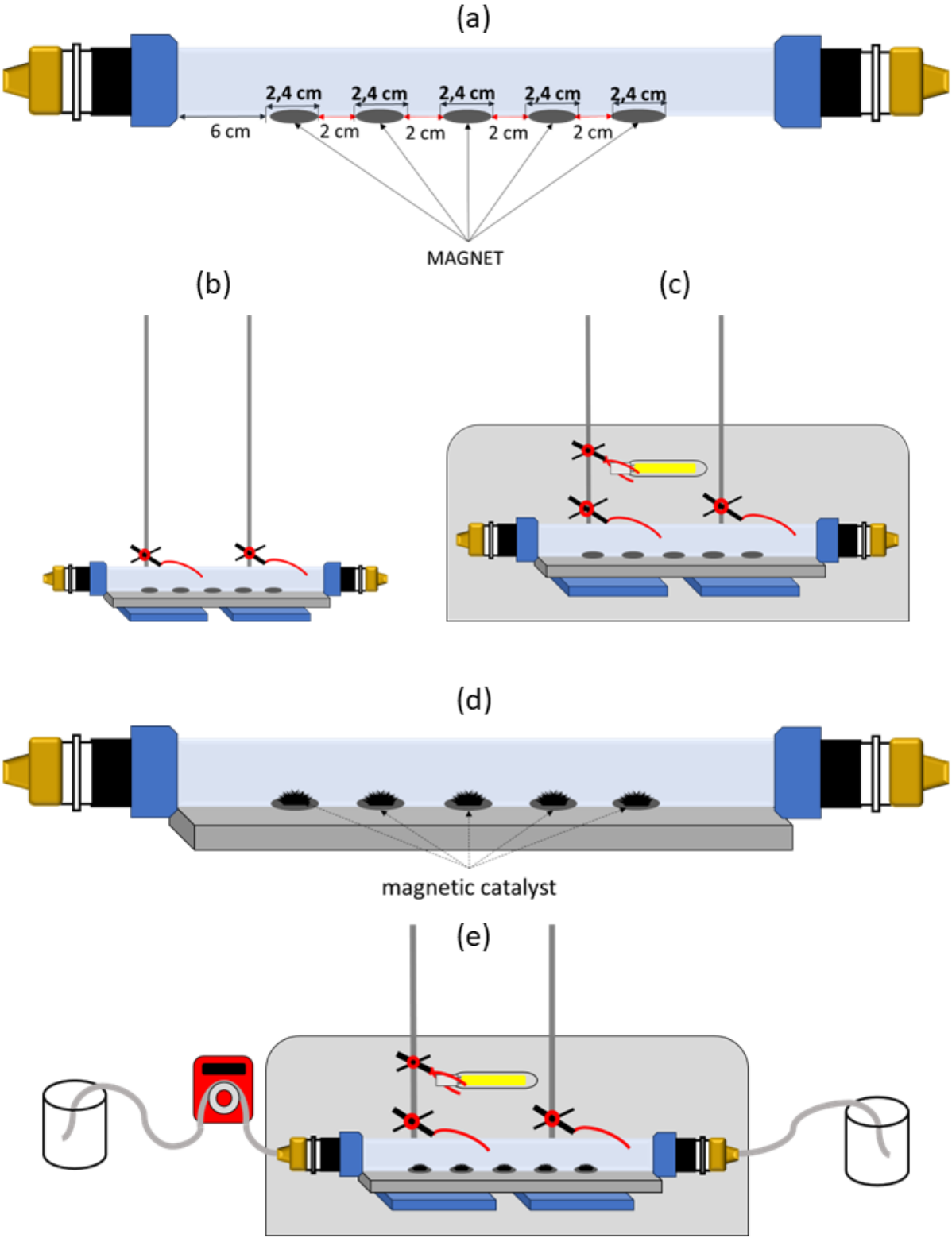

Figure 1. Illustration of the process of assembling the system to perform photocatalysis: (**a**) establishing the distance between the magnets along the reactor; (**b**) fixing the reactor on the support; (**c**) coupling the mercury lamp and protecting it so as not to lose light during the process; (**d**) placement of the catalyst, which was "fixed" by magnetic attraction to the external magnet; (**e**) placement of the inlet and outlet hoses in the reactor; the inlet hose leaving the solution containing the pollutant passes through the peristaltic pump to control the flow.

Figure 2. Catalyst immobilization on aggregated flower-like structures.

3. Results and Discussion

3.1. Characterization Techniques

The following characterizations were discussed in detail by Oliveira et al. (2023) [17]; in this work, important points were revisited for a better understanding [1].

The GAP energy values of CFNb are 3.12 eV (linear method) and 3.20 eV (derivative method). CFNb has a pHPZC value of around 6.9. The SEM image analysis makes it possible to observe clusters of nanomaterials, which are typical of materials with magnetic properties [7–10,12,13]. Energy dispersive spectroscopy (EDS), which allows the detection and fraction of chemical elements on the surface, reveals the fraction of each component and is summarized in weight: 33.6% is oxygen, 27.3% is iron, 24.8% is niobium, and 14% is cobalt.

In the interpretation of the XRD analysis, the peaks were identified as cobalt ferrite and niobium pentoxide. Further exploring the results of the XRD characterization, the average crystallite sizes (L) were calculated using Scherrer's Equation, obtaining the size of 24.10 nm for CFNb nanoparticles. In the TEM image, the nanoparticle does not demonstrate a regular shape, but it is possible to conclude that the cobalt ferrite was synthesized in a niobium oxide structure. Using resources such as ImageJ to interpret the size of CFNb particles, the average particle size was calculated to be around 32.9 $\pm$ 3.5 nm. The value of the average particle size is not so far from that found using XRD.

According to the VSM characterization, CFNb nanoparticles have a ferromagnetic behavior with saturation magnetization (Ms) estimated at 26.5 emu/g, with remanent magnetization (Mr) of approximately 10.7 emu/g, and a coercivity (Hc) of around 844 Oe; Figure 3. The literature does not have the same compound to compare. We need to consider the calcined temperature used in the cobalt ferrite synthesis because this factor has a strong influence on the results. Senthil et al. obtained the values of the Ms and Hc at 23 emu/g and 900 Oe, respectively, to cobalt ferrite synthesized at 873 K [20]. El-Okr et al. obtained to cobalt ferrite synthesized at 773 K and 973 K and obtained the following values: Ms between 36 and 42.38 emu/g, Mr 8.0−16.5 emu/g, and Hc 400–650 Oe, respectively [21].

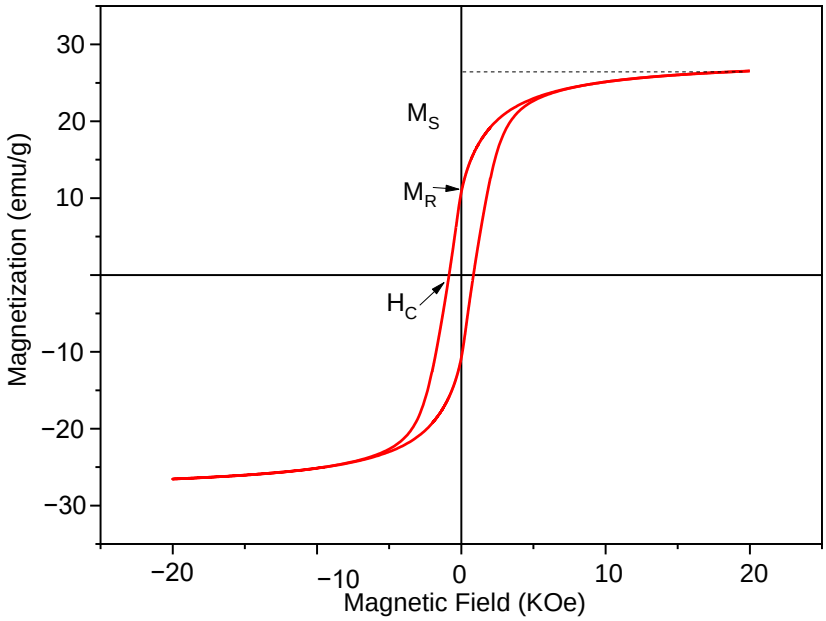

Figure 3. Vibrating Sample Magnetometer graph CFNb sample.

3.2. Continuous Process

Few articles are found simultaneously involving the topics "continuous flow catalysis" and "degradation"; just twelve were found on the Web of Science until this research. And if you try to include "paracetamol" or "emerging pollutants", nothing is found. This is because carrying out a catalysis reaction in continuous flow has some difficulties, the biggest of which is keeping the catalysts fixed while contaminating effluent flows. With magnetic catalysts, this is possible by placing magnets externally at strategic points throughout the reactor. This difficulty is linked to the catalysis itself because if membranes were placed to "hold" the catalyst, adsorption by the membranes could make the catalysis evaluation difficult since the effluent would not be in direct contact with the catalyst.

However, the main advantages of using the continuous process according to Binjhade et al. (2022) are scalability, the continuous monitoring of reactions, and efficiency [22]. In this context, the continuous process experiments evaluated some process parameters: pH, flow rate (residence time), photolysis, and adsorption.

3.3. pH Influence

To analyze the effect of pH, tests were carried out with the pH of the solution (without adjustments—pH 6.3) and at an acidic pH (2.5). The results indicated that a decrease in pH had a positive effect on the degradation of paracetamol. There was an increase in pollutant removal of around 50%. The results are indicated in Figure 4. According to Sajid et al. (2022), the adsorption capacity and the drug removal efficiency in the material is generally influenced by the pH of the system [23]. Previous results indicated a pH_{PZC} value of around 6.9 for the pH_{PZC} catalyst [17]. This value indicates that the catalyst positively charged ($pH < pH_{PZC}$). The results described in the literature using the batch process indicated that a pH of 2.59 and a catalyst concentration of 441.41 mg·L^{-1} was efficient to completely degrade paracetamol [17,24]. On the other hand, Yang et al. (2008) studied the degradation of paracetamol with the TiO_2 catalyst and showed that the rate constant increases slightly with an increasing pH up to 9.5 [25]. This was attributed to enhanced •OH formation, because at a high pH, more hydroxide ions available on the TiO_2 surface can be easily oxidized and form more •OH.

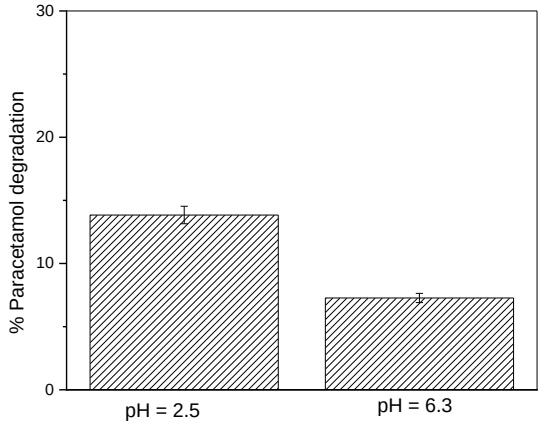

Figure 4. pH influence on paracetamol removal [flow rate= 5.77 mL·min^{-1}; 40 rpm].

3.4. Effect of Flow Rate

To evaluate the most appropriate residence time for paracetamol degradation, different flow rates were defined for the effluent, at 20, 40, and 60 mL min^{-1}. These flow rates are used according to the limitations of the equipment (peristaltic pump). The results indicated that a longer residence time favors the degradation of paracetamol (~27%, 20 mL·min^{-1}) due to an increase in the effluent—catalyst contact time. On the other hand, as the flow rate increases (from 40 to 60 mL·min^{-1}), there is a tendency for it to stabilize. Studies in batch processes indicate, with the same catalyst, a paracetamol removal of 97.5% in 60 min [17]. Other batch reactor studies also indicated efficiency in paracetamol mineralization at pH 3.0 and 10.0:33% and 76% without H_2O_2, and at 69% and 67% with 33 mg·L^{-1} H_2O_2 for P 25 [26]. However, observing that the residence time in the continuous reactor, the values obtained in the paracetamol degradation were approximately 23% (2.84 mL min^{-1}, 20 rpm), 12% (5.77 L min^{-1}, 40 rpm), and 10% (8.63 mL min^{-1}, 60 rpm); Figure 5.

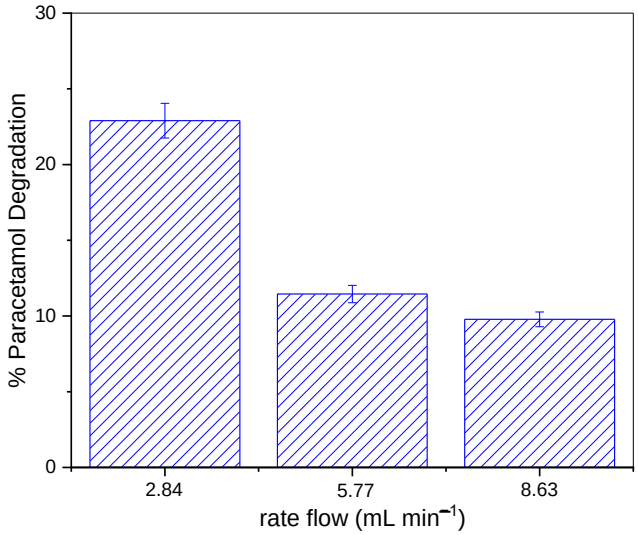

Figure 5. Paracetamol removal results in a continuous flow.

3.5. Effect of Catalyst Utilization Cycles

To evaluate the reuse of the catalyst, residence time was used. The results indicated that for the residence time using the flow rate of 20 mL min^{-1}, no significant changes were observed in the degradation of paracetamol at around 23% (Figure 6a). However, when we increase the flow rate to 60 mL min^{-1}, a more turbulent process occurs; there is a consequent decrease in the effluent-catalyst contact time, and there is a tendency for a decrease in degradation. Despite this, at an intermediate flow rate, instability occurs.

The EDS results before (Figure 6b) and after (Figure 6c) the tests indicated that the amount of iron remained constant, before and after the test. For niobium, there was a decrease. Despite being a one-off analysis, it can be seen that the catalyst remained fixed in the reactor through magnetization. Furthermore, the release of small white particles, possibly niobium, was observed at the beginning of the test.

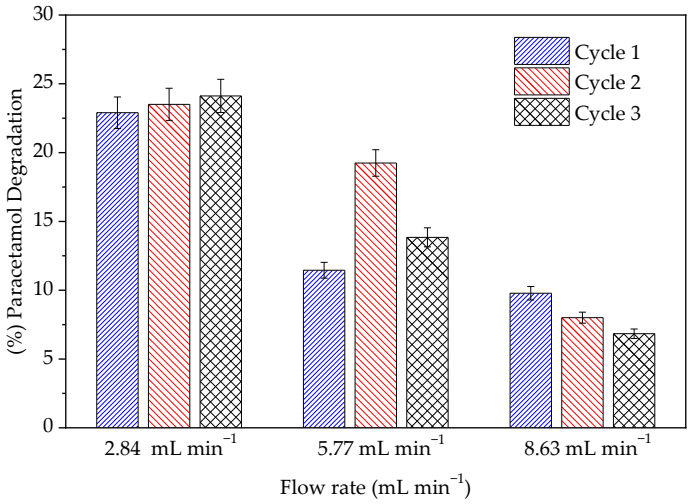

(**a**)

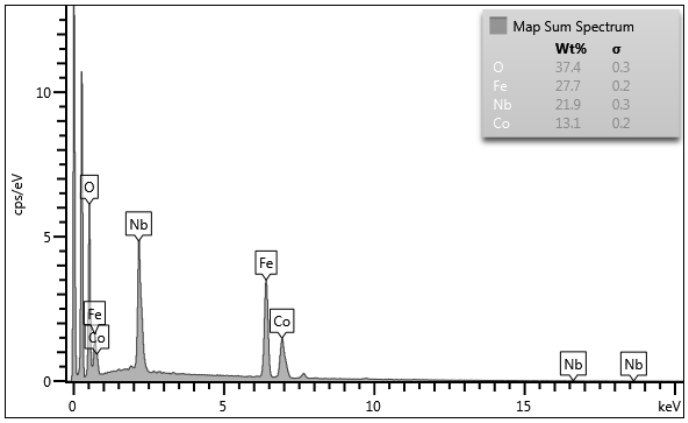

(**b**)

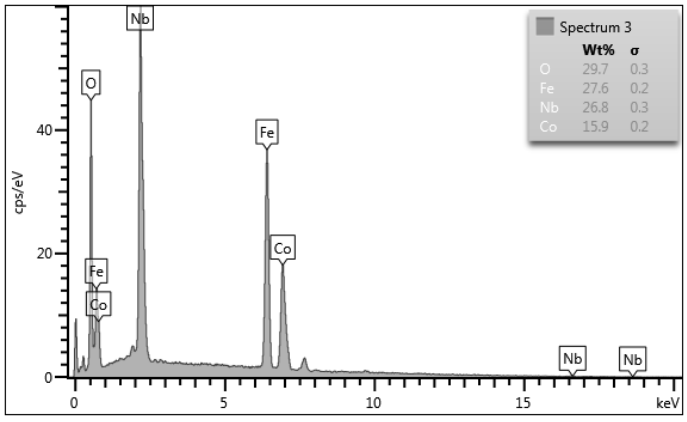

(**c**)

Figure 6. (**a**) Influence of residence time on paracetamol removal cycles [pH 2.5]; (**b**) EDS before test; (**c**) EDS after test.

Considering a statistical analysis using the ANOVA test, the results indicated that there is a significant effect on the degradation of paracetamol at the flow rates studied. This effect can be demonstrated in Figure 7. A p-value lower than 0.05 was obtained, which indicates a significant difference in the degradation percentage for different flow rates in the experimental tests.

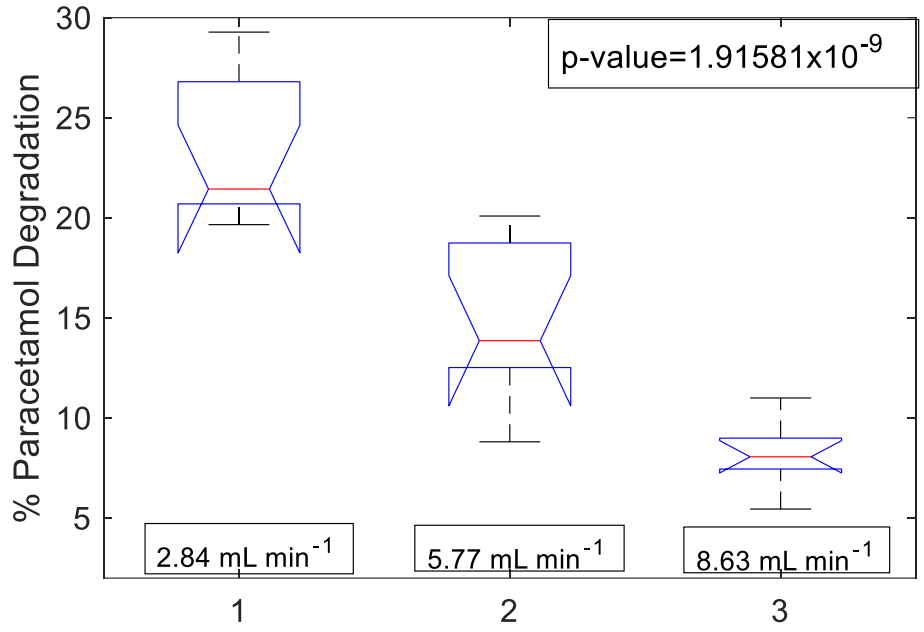

Figure 7. Results of Pareto chart.

3.6. Photolysis and Adsorption

Photolysis was also evaluated by residence time and flow rate. It was observed that the results obtained, even at low flow rates, were not so different from those obtained at high flows. At the lowest flow, the values were between 8 and 6.0%; at the intermediate flow rate, they were between 3.3–2.2%, and at the highest flow rate, they were between 1.8–2.6% in the degradation of paracetamol via photolysis (Figure 8a). The results obtained in the adsorption test were also very close, independently of the flow rate used (Figure 8b). Yang et al. (2008) observed a significant reduction in paracetamol concentration during irradiation with UVC radiation alone, demonstrating the effects of photolysis [25]. On the other hand, only irradiation indicated the ineffective mineralization of paracetamol in the absence of a catalyst. As can be seen in Figure 8b, changes in flow did not significantly alter the amount of paracetamol adsorbed on the catalytic surface; the adsorption rate was approximately 10%.

The work was carried out because it was considered relevant to synergistically approach the themes of emerging pollutants, catalysis, and continuous flow. Related to effluent treatment through catalysis, this work fits into the principles of green chemistry (specifically 9—catalysis and 11—real-time analysis for pollution prevention) [4] and the UN Sustainable Development Goals (specifically 6—clean water and sanitation and 14—life below water) [27]. It can be one more alternative to promote sustainability through little daily attitudes.

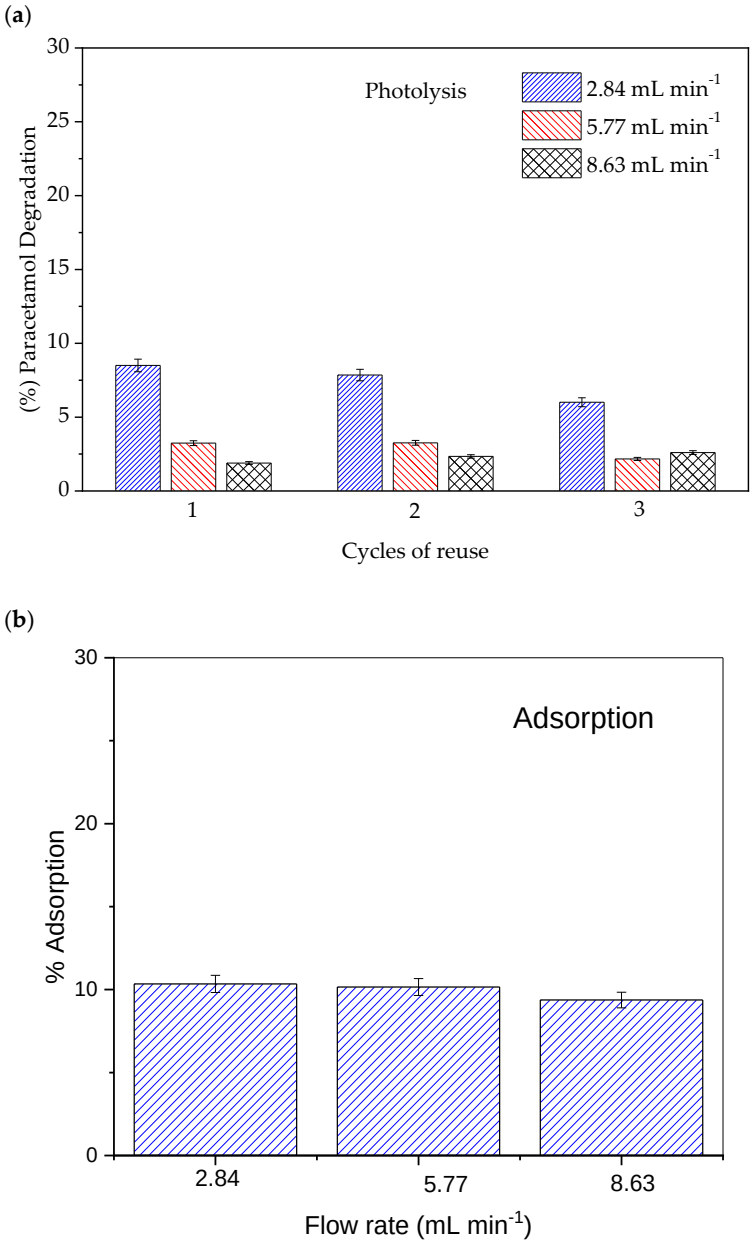

Figure 8. Paracetamol (**a**) degradation via photolysis test; and (**b**) removal using adsorption test.

4. Conclusions

The results indicated that the degradation of paracetamol can be carried out via a continuous photocatalytic process. The magnetic immobilization of the catalyst was adequate, because the catalyst leaching did not occur with increasing flow. The study of the parameters indicated that pH influences the degradation of the pollutant. Photolysis and adsorption indicated that the flow rate and residence time were not significant. In reuse cycles, the drop in catalytic activity is more pronounced at higher flow rates. At low flow rates in three cycles, a slight decrease in catalytic activity is observed.

Considering the limitations such as time, the amount of pollutant for analysis, the amount of catalyst available, and the lack of parameters for direct comparison, among others, this research was carried out based on the best result obtained for degradation in batch reaction, using the same catalyst. This research is relevant as it opens up many possibilities for future work where different conditions of pH, flow, the amount of catalyst, and the distance between magnets (catalysts), among other parameters, can be explored.

Author Contributions: J.R.P.O., E.A., M.E.K.F. and E.T.d.P. methodology and investigation M.Z.F., R.B., O.C.A., G.G.L. and A.M.T. conceived, writing—review and editing. All authors discussed the results and contributed to the final manuscript. All authors have read and agreed to the published version of the manuscript.

Funding: This research was funded by CNPq project 304068/2022-5.

Institutional Review Board Statement: Not applicable.

Informed Consent Statement: Not applicable.

Data Availability Statement: Data are contained within the article.

Acknowledgments: The authors thank the CBMM-Companhia Brasileira de Metalurgia e Mineração by the Niobium, and CNPq agency.

Conflicts of Interest: The authors declare no conflicts of interest.

References

1. Islam, M.A.; Nazal, M.K.; Sajid, M.; Altahir Suliman, M. Adsorptive Removal of Paracetamol from Aqueous Media: A Review of Adsorbent Materials, Adsorption Mechanisms, Advancements, and Future Perspectives. *J. Mol. Liq.* **2024**, *396*, 123976. [CrossRef]
2. Alobaidi, R.A.K.; Ulucan-Altuntas, K.; Mhemid, R.K.S.; Manav-Demir, N.; Cinar, O. Biodegradation of Emerging Pharmaceuticals from Domestic Wastewater by Membrane Bioreactor: The Effect of Solid Retention Time. *Int. J. Environ. Res. Public. Health* **2021**, *18*, 3395. [CrossRef] [PubMed]
3. Roslan, N.N.; Lau, H.L.H.; Suhaimi, N.A.A.; Shahri, N.N.M.; Verinda, S.B.; Nur, M.; Lim, J.-W.; Usman, A. Recent Advances in Advanced Oxidation Processes for Degrading Pharmaceuticals in Wastewater—A Review. *Catalysts* **2024**, *14*, 189. [CrossRef]
4. Anastas, P.; Warner, J. 12 Principles of Green Chemistry. Available online: https://www.acs.org/content/acs/en/greenchemistry/principles/12-principles-of-green-chemistry.html (accessed on 20 January 2024).
5. Borges, M.; García, D.; Hernández, T.; Ruiz-Morales, J.; Esparza, P. Supported Photocatalyst for Removal of Emerging Contaminants from Wastewater in a Continuous Packed-Bed Photoreactor Configuration. *Catalysts* **2015**, *5*, 77–87. [CrossRef]
6. Soltys, L.; Olkhovyy, O.; Tatarchuk, T.; Naushad, M. Green Synthesis of Metal and Metal Oxide Nanoparticles: Principles of Green Chemistry and Raw Materials. *Magnetochemistry* **2021**, *7*, 145. [CrossRef]
7. Wei, X.; Naraginti, S.; Chen, P.; Li, J.; Yang, X.; Li, B. Visible Light-Driven Photocatalytic Degradation of Tetracycline Using p-n Heterostructured Cr_2O_3/ZrO_2 Nanocomposite. *Water* **2023**, *15*, 3702. [CrossRef]
8. Savun-Hekimoğlu, B.; Eren, Z.; Ince, N.H. Photocatalytic Destruction of Caffeine on Sepiolite-Supported TiO_2 Nanocomposite. *Sustainability* **2020**, *12*, 10314. [CrossRef]
9. Amini, M.; Hosseini, S.M.P.; Chaibakhsh, N. High-Performance $NiO@Fe_3O_4$ Magnetic Core–Shell Nanocomposite for Catalytic Ozonation Degradation of Pharmaceutical Pollution. *Environ. Sci. Pollut. Res.* **2023**, *30*, 98063–98075. [CrossRef] [PubMed]
10. Masunga, N.; Mamba, B.B.; Kefeni, K.K. Magnetically Separable Samarium Doped Copper Ferrite-Graphitic Carbon Nitride Nanocomposite for Photodegradation of Dyes and Pharmaceuticals under Visible Light Irradiation. *J. Water Process Eng.* **2022**, *48*, 102898. [CrossRef]
11. Malefane, M.E.; Feleni, U.; Kuvarega, A.T. Cobalt (II/III) Oxide and Tungsten (VI) Oxide p-n Heterojunction Photocatalyst for Photodegradation of Diclofenac Sodium under Visible Light. *J. Environ. Chem. Eng.* **2020**, *8*, 103560. [CrossRef]
12. Alvarado-Rolon, O.; Natividad, R.; Ramírez-García, J.; Orozco-Velazco, J.; Hernandez-Servin, J.A.; Ramírez-Serrano, A. Kinetic Modelling of Paracetamol Degradation by Photocatalysis: Incorporating the Competition for Photons by the Organic Molecule and the Photocatalyst. *J. Photochem. Photobiol. A Chem.* **2021**, *412*, 113252. [CrossRef]
13. Rossi, S.; Herbrik, F.; Resta, S.; Puglisi, A. Supported Eosin Y as a Photocatalyst for C-H Arylation of Furan in Batch and Flow. *Molecules* **2022**, *27*, 5096. [CrossRef] [PubMed]
14. Nour, M.M.; Tony, M.A. The Environmental Oxidation of Acetaminophen in Aqueous Media as an Emerging Pharmaceutical Pollutant Using a Chitosan Waste-Based Magnetite Nanocomposite. *Resources* **2024**, *13*, 47. [CrossRef]
15. Çako, E.; Gunasekaran, K.D.; Rajendran, S.; Zielińska-Jurek, A. Recent Advances on Magnetic Carbon-Related Materials in Advanced Oxidation Processes of Emerging Pollutants Degradation. *Water Resour. Ind.* **2024**, *31*, 100241. [CrossRef]
16. Hermosilla, D.; Han, C.; Nadagouda, M.N.; Machala, L.; Gascó, A.; Campo, P.; Dionysiou, D.D. Environmentally Friendly Synthesized and Magnetically Recoverable Designed Ferrite Photo-Catalysts for Wastewater Treatment Applications. *J. Hazard. Mater.* **2020**, *381*, 121200. [CrossRef] [PubMed]
17. Oliveira, J.R.P.; Ribas, L.S.; Napoli, J.S.; Abreu, E.; Diaz de Tuesta, J.L.; Gomes, H.T.; Tusset, A.M.; Lenzi, G.G. Green Magnetic Nanoparticles $CoFe_2O_4@Nb_5O_2$ Applied in Paracetamol Removal. *Magnetochemistry* **2023**, *9*, 200. [CrossRef]
18. Ibrahim, I.; Belessiotis, G.V.; Arfanis, M.K.; Athanasekou, C.; Philippopoulos, A.I.; Mitsopoulou, C.A.; Romanos, G.E.; Falaras, P. Surfactant Effects on the Synthesis of Redox Bifunctional V_2O_5 Photocatalysts. *Materials* **2020**, *13*, 4665. [CrossRef]
19. Oliveira, M.; Santos, V.G.; Carvalho, L.S.; Ruiz, D.; Silva Barbosa, I.A.; Das Virgens, C.F.; Martins, A.R. Adsorbents Obtained from Black Liquor Residues: Synthesis, Characterization, and Evaluation in the Removal of Textile Dyes. *Sci. Plena* **2021**, *16*, 12. [CrossRef]

20. Senthil, V.P.; Gajendiran, J.; Raj, S.G.; Shanmugavel, T.; Ramesh Kumar, G.; Parthasaradhi Reddy, C. Study of Structural and Magnetic Properties of Cobalt Ferrite ($CoFe_2O_4$) Nanostructures. *Chem. Phys. Lett.* **2018**, *695*, 19–23. [CrossRef]
21. El-Okr, M.M.; Salem, M.A.; Salim, M.S.; El-Okr, R.M.; Ashoush, M.; Talaat, H.M. Synthesis of Cobalt Ferrite Nano-Particles and Their Magnetic Characterization. *J. Magn. Magn. Mater.* **2011**, *323*, 920–926. [CrossRef]
22. Binjhade, R.; Mondal, R.; Mondal, S. Continuous Photocatalytic Reactor: Critical Review on the Design and Performance. *J. Environ. Chem. Eng.* **2022**, *10*, 107746. [CrossRef]
23. Sajid, M.; Bari, S.; Saif Ur Rehman, M.; Ashfaq, M.; Guoliang, Y.; Mustafa, G. Adsorption Characteristics of Paracetamol Removal onto Activated Carbon Prepared from Cannabis Sativum Hemp. *Alex. Eng. J.* **2022**, *61*, 7203–7212. [CrossRef]
24. Fuziki, M.E.K.; Brackmann, R.; Dias, D.T.; Tusset, A.M.; Specchia, S.; Lenzi, G.G. Effects of Synthesis Parameters on the Properties and Photocatalytic Activity of the Magnetic Catalyst $TiO_2/CoFe_2O_4$ Applied to Selenium Photoreduction. *J. Water Process Eng.* **2021**, *42*, 102163. [CrossRef]
25. Yang, L.; Yu, L.E.; Ray, M.B. Degradation of Paracetamol in Aqueous Solutions by TiO_2 Photocatalysis. *Water Res.* **2008**, *42*, 3480–3488. [CrossRef]
26. Zhou, Y.; Liu, Q.; Li, X.; Ling, L.; Zhou, Y. Efficient Oxidation of Paracetamol Triggered by Molecular-Oxygen Activation at B-Cyclodextrin-Modified Titanate Nanotubes. *Chem. Asian J.* **2022**, *17*, e202200352. [CrossRef]
27. United Nations Development Programme the Sdgs in Action. Available online: https://www.undp.org/sustainable-development-goals?gclid=Cj0KCQjwnrmlBhDHARIsADJ5b_njdNkJH46XlfGzeft_s8lwrll8WsqfeBfcvkkX4xuHFeYD0LKDz64aAhUiEALw_wcB (accessed on 12 July 2023).